



Full length article

A teleostan homolog of catalase from black rockfish (*Sebastes schlegelii*): Insights into functional roles in host antioxidant defense and expressional responses to septic conditions



Don Anushka Sandaruwan Elvitigala^{a, b}, Thanthrige Thiunuwan Priyathilaka^{a, b},
Ilsong Whang^b, Bo-Hye Nam^c, Jehee Lee^{a, b, *}

^a Department of Marine Life Sciences, School of Marine Biomedical Sciences, Jeju National University, Jeju Self-Governing Province 690-756, Republic of Korea

^b Fish Vaccine Research Center, Jeju National University, Jeju Special Self-Governing Province 690-756, Republic of Korea

^c Biotechnology Research Division, National Fisheries Research and Development Institute, 408-1 Sirang-ri, Gijang-up, Gijang-gun, Busan 619-705, Republic of Korea

ARTICLE INFO

Article history:

Received 18 November 2014

Received in revised form

10 February 2015

Accepted 12 February 2015

Available online 20 February 2015

Keywords:

Catalases

Black rockfish

Antioxidant properties

Immune challenge

Transcriptional analysis

ABSTRACT

Antioxidative defense renders a significant protection against environmental stress in organisms and maintains the correct redox balance in cells, thereby supporting proper immune function. Catalase is an indispensable antioxidant in organisms that detoxifies hydrogen peroxides produced in cellular environments. In this study, we sought to molecularly characterize a homolog of catalase (RfCat), identified from black rockfish (*Sebastes schlegelii*). *RfCat* consists of a 1581 bp coding region for a protein of 527 amino acids, with a predicted molecular weight of 60 kD. The protein sequence of RfCat harbored similar domain architecture to known catalases, containing a proximal active site signature and proximal heme ligand signature, and further sharing prominent homology with its teleostan counterparts. As affirmed by multiple sequence alignments, most of the functionally important residues were well conserved in RfCat. Furthermore, our phylogenetic analysis indicates its common vertebrate ancestral origin and a close evolutionary relationship with teleostan catalases. Recombinantly expressed RfCat demonstrated prominent peroxidase activity that varied with different substrate and protein concentrations, and protected against DNA damage. *RfCat* mRNA was ubiquitously expressed among different tissues examined, as detected by qPCR. In addition, *RfCat* mRNA expression was modulated in response to pathogenic stress elicited by *Streptococcus iniae* and poly I:C in blood and spleen tissues. Collectively, our findings indicate that RfCat may play an indispensable role in host response to oxidative stress and maintain a correct redox balance after a pathogen invasion.

© 2015 Elsevier Ltd. All rights reserved.

1. Introduction

Reactive oxygen species (ROS) play an indispensable role in host anti-microbial defense, acting directly or as signaling molecules in host inflammatory or innate immune responses [1–4]. Nevertheless, excessive ROS generation can have detrimental effects, including host cell damage due to oxidation of biomolecules, DNA mutagenesis, activation of pro-cell death factors, and tumorigenesis [5–7].

Moreover, accumulation of ROS in cellular environments can compromise host immunity [8]. Therefore, a proper ROS balance must be maintained for survival. This balance is regulated by the cellular antioxidant system, consisting of ROS scavengers, such as the enzymes catalase, superoxide dismutase (SOD), glutathione peroxidase (Gpx), thioredoxin, thioredoxin reductase (TrxR), and peroxiredoxins (Prx) [9] along with non-enzyme constituents, including glutathione, vitamin A, E, and C [10]. Among enzymatic components, catalase plays an indispensable role in detoxifying hydrogen peroxide to form the nontoxic end-products water and oxygen [9]. Generally, two types of catalases are found in organisms, classical Fe heme enzymes and catalase-peroxidases. The former belongs to a small group of manganese enzymes, whereas the latter contains a covalent triplet of distal side chains, which catalyze peroxidatic and catalytic reactions

* Corresponding author. Marine Molecular Genetics Lab, Department of Marine Life Sciences, College of Ocean Science, Jeju National University, 66 Jejudaehakno, Ara-Dong, Jeju 690-756, Republic of Korea. Tel.: +82 64 754 3472; fax: +82 64 756 3493.

E-mail address: jehee@jejunu.ac.kr (J. Lee).

following a different mechanism than the classical heme enzymes [11]. In addition to hydrogen peroxide, catalase can also breakdown several other substrates, including phenol, methanol, ethanol, and nitrites [12]. Interestingly, catalase is an efficient enzyme with a high turn-over rate; each second, one catalase molecule can convert millions of peroxide molecules into water and oxygen [13].

Catalase is ubiquitously expressed in prokaryotes and eukaryotes, consisting of four identical subunits of 50–60 kD [14,15]. Each monomeric subunit contains a single heme group and NADPH molecule on its surface [16,17]. This NADPH prevents the enzyme from oxidation by its own substrate. Much of the information on catalase, especially regarding its structure and the regulation of its expression, has been reported in mammals [18,19], plants [20], and bacteria [21]. Human catalase is a member of the peroxisomal glycoprotein family with four subunits, each harboring four conceptual domains, including β -barrel, N-terminal threading arm, wrapping loop, and C-terminal helices [22].

There are some credible evidences which suggest that catalase can mediate host immune responses, besides its main ROS scavenging role in cells. For instance, *Caenorhabditis elegans* catalase was found to stimulate innate immune gene response [23], and catalase was shown to mediate a main host defense system required in host–microbe interactions in the gastrointestinal tract of fruit flies [24]. In addition, catalase activity and/or expression was shown to be altered by viral infections in crustaceans [25–28], and enhanced *catalase* transcription was detected in mollusks with bacterial infection [29,30]. Hence, gaining insight into different counterparts of catalase in different taxons is essential to understand its potential, but unrevealed roles in organisms.

Information on lower vertebrate catalase homologues, especially of teleost origin, is relatively scarce. Among fish catalases, both rock bream (*Oplegnathus fasciatus*) [31] and zebrafish (*Danio rerio*) [32,33] have been evaluated to date. According to these reports, teleostan catalases demonstrated a strong peroxidase activity at a broad spectrum of temperatures and pH conditions, and its expression can be modulated by pathogen invasion. In addition, another study showed that gene expression of catalase can be temporarily induced by starvation in rock breams [34].

Mariculture is considered as a productive way to increase marine fish and shellfish production. Therein, fish and shellfish are cultured at a high density, either in an enclosed section of ocean or in tanks filled with seawater. Therefore, these creatures are more susceptible to environmental stress factors, including pathogen infections, which can negatively affect their survival and growth. Moreover, oxidative stress in these species can suppress their immune response, and in turn make them more vulnerable to infections [35]. Therefore, gaining insight into molecular defense mechanisms against stress is a primary step for the development of sustainable mariculture, by identifying targets for potential therapies. Since catalase is an important antioxidant and a relevant immune molecule, we sought to identify and molecularly characterize its homolog in black rockfish (*Sebastes schlegelii*), which is an economically important and mariculturally farmed comestible, especially in the Asia Pacific region.

In the present study, a teleostan homolog of catalase (RfCat) was identified from black rockfish and characterized at the molecular level, providing evidence for molecular expression during pathogenic stress, along with its putative functional roles against oxidative defense.

2. Materials and methods

2.1. Black rockfish cDNA database

A database of black rockfish cDNA sequences was created by 454 GS-FLX™ sequencing technique [36]. In brief, the total RNA was

extracted from blood, liver, head kidney, gill, intestine, and spleen tissues from three fish (~100 g) challenged with immune stimulants including *Edwardsiella tarda* (10^7 CFU/fish), *Streptococcus iniae* (10^7 CFU/fish), lipopolysaccharide (1.5 mg/fish), polyinosinic:polycytidylic acid (poly I:C, 1.5 mg/fish). The extracted RNA was then cleaned using an RNeasy Mini kit (Qiagen, USA) and assessed for quality and quantified using an Agilent 2100 Bioanalyzer (Agilent Technologies, Canada), resulting in an RNA integration score (RIN) of 7.1. Subsequently, the GS-FLX™ 454 shotgun library was constructed, and a cDNA database was established using fragmented RNA (average size – 1147 bp) from the aforementioned RNA samples (Macrogen, Korea).

2.2. Identification and sequence characterization of RfCat

We identified the complete cDNA sequence of *RfCat* from the black rockfish cDNA database using the Basic Local Alignment Search Tool (BLAST) algorithm (<http://blast.ncbi.nlm.nih.gov/Blast.cgi>). Then, the identified sequence was characterized using different bioinformatics tools. The full-length putative coding sequence of *RfCat* was identified, and the corresponding amino acid sequence was derived using DNAsist 2.2 software. Domain architecture corresponding to the derived primary structure of RfCat was predicted using ExpAsy Prosite database (<http://prosite.expasy.org>). Moreover, some of the physicochemical properties of the derived protein sequence were determined by the ExpAsy ProtParam tool (<http://web.expasy.org/protparam>). Comparison of the RfCat protein sequence with its homologues was carried out through pairwise and multiple sequence alignments, executed by Matgat software [37] and ClustalW2 (<http://www.Ebi.ac.uk/Tools/clustalw2>) program, respectively. The phylogenetic reconstruction of RfCat was generated according to the neighbor-joining method using Molecular Evolutionary Genetics Analysis (version 4.0) software (MEGA 4.0) [38], validated by 1000 bootstrap replications. In addition, the tertiary structure of RfCat was modeled by the I-TASSER online server [39,40] and visualized using PyMOL 1.7 program (<http://www.pymol.org>).

2.3. Overexpression and purification of recombinant RfCat (rRfCat)

rRfCat was expressed as a fusion protein with maltose binding protein (MBP) as previously described, but with some modifications [41]. Briefly, the coding sequence of *RfCat* was amplified using the sequence-specific primer pair, RfCat-F and RfCat-R, which contained restriction enzyme sites for *EcoRI* and *Sall*, respectively (Table 1). PCR was performed in a TaKaRa thermal cycler (TaKaRa, Otsu, Shiga, Japan) in a total volume of 50 μ L, containing 5 U TaKaRa ExTaq polymerase, 5 μ L of $10\times$ TaKaRa ExTaq buffer, 8 μ L 2.5 mM dNTPs, 80 ng of template, and 40 pmol of each primer (Table 1). The PCR was performed under the following conditions: initial denaturation at 94 °C for 3 min, followed by 35 cycles of 94 °C for 30 s, 57 °C for 30 s, and 72 °C for 1 min, with a final extension at 72 °C for 5 min. The PCR product (~1.6 kbp) was resolved on a 1% agarose gel, excised, and purified using the Expin™ Gel SV kit (GeneAll, Korea). Digested pMAL-c2X vector (150 ng) and the PCR product (108 ng) were ligated using Mighty Mix (5.0 μ L; TaKaRa) at 4 °C overnight. The ligated pMAL-c2X/RfCat product was transformed into DH5 α cells and sequenced. After sequence conformation, the recombinant expression plasmid was transformed into *Escherichia coli* BL21 (DE3) competent cells. Expression of the rRfCat fusion protein was induced using isopropyl- β -D-galactopyranoside (IPTG, 0.5 mM). *E. coli* BL21 cells were grown in 500 mL Luria broth (LB) supplemented with ampicillin (100 μ g/mL) and glucose (0.2%) at 20 °C for 9 h. Induced *E. coli* BL21 (DE3) cells were then cooled on ice for 30 min and harvested by centrifugation at 3500 rpm for 30 min at

Table 1
Primers used in this study.

Name	Purpose	Sequence (5' → 3')
RfCat-qF	qPCR of <i>RfCat</i>	CTTCATCAAGGACGCCATGCTGTT
RfCat-qR	qPCR of <i>RfCat</i>	TAGCCGTTTCATGTGACGGAATCCA
RfCat-F	Amplification of coding region (<i>EcoRI</i>)	GAGAGaattcATGGCTGAAAACAGAGATAAAGCTTCGG
RfCat-R	Amplification of coding region (<i>Sall</i>)	GAGAGAgctgacTCACATCTTGGAGGACGCGGC
RfEF1A-F	qPCR for black rockfish EF1A	AACCTGACCACTGAGGTGAAGTCTG
RfEF1A-R	qPCR for black rockfish EF1A	TCCTTGACGGACAGTCTTGTATGTT

4 °C. Harvested cells were resuspended in 20 mL of column buffer (20 mM Tris–HCl pH 7.4 and 200 mM NaCl) and stored at –20 °C. *E. coli* cells were thawed and lysed in column buffer using cold sonication. The protein was then purified using the pMAL™ Protein Fusion and Purification System (New England BioLabs, Beverly, MA, USA). The purified protein was eluted using an elution buffer (10 mM maltose in column buffer). Its concentration was determined by the Bradford method using bovine serum albumin as a standard [42]. The purified fusion protein (rRfCat) was then assayed for peroxidase activity and the ability to inhibit oxidative DNA damage. Samples collected at different steps of the rRfCat purification were analyzed by 12% sodium dodecyl sulfate polyacrylamide gel electrophoresis (SDS-PAGE) using standard protein size markers (Enzyomics, Korea) under reducing conditions. The gel was stained with 0.05% Coomassie blue R-250 and observed followed by a standard destaining procedure.

2.4. Peroxidase activity assay

The peroxidase activity of RfCat was analyzed using the purified recombinant fusion protein using varying enzyme and substrate concentrations, according to a previously described method [43] with some modifications. To determine the effect of enzyme concentration on peroxidase activity, 50 µL of rRfCat containing different amounts of protein was mixed with 70 µL of citrate–phosphate buffer (0.1 M, pH 5) and 20 µL H₂O₂ (10 mM) in a 96-well plate. After mixing, the plate was incubated at 25 °C for 5 min. To determine the remaining amount of H₂O₂, 30 µL of 2,2'-azino-bis(3-ethylbenzothiazoline-6-sulphonic acid) (ABTS) and peroxidase (1 U/mL) were added to the reaction mixtures, with an additional incubation at 37 °C for 10 min. Finally, the developed blue-green color due to the formation of ABTS cation was measured at 405 nm using a multi-plate reader (Thermo Scientific, Waltham, MA, USA). The same assay protocol was followed to determine the effect of substrate (H₂O₂) concentration on rRfCat peroxidase activity. The same volume of H₂O₂ with varying concentrations was used to assay the activity of 50 µg/mL final concentration of recombinant protein. In both experiments, peroxidase activity was expressed as the percent relative activity to the negative control assay performed without the protein, as the mean of three assays. Additional control assays were also performed with maltose binding protein (MBP) instead of rRfCat to determine whether the MBP fusion protein affected peroxidase activity.

2.5. Determination of oxidative DNA damage

To determine the potential protective effect of RfCat against oxidative DNA damage, a thiol mixed-function oxidation (MFO) assay [44] was performed in the presence of rRfCat or MBP (control) in reaction medium, with some modifications. Briefly, a reaction mixture containing 40 µM Fe (III) chloride, 10 mM dithiothreitol (DTT), and 25 mM HEPES (pH 7.0) was incubated with rRfCat (10 µg) or MBP (10 µg), or without any protein, for 10 min at 25 °C. Subsequently, 1 µg of pUC19 plasmid DNA was added to each mixture

and incubated at 37 °C for 10 min to induce DNA breakage through the formation of hydroxyl radicals. Immediately after the incubation period, the DNA in each reaction mixture was purified using AccuPrep® PCR purification kit (Bioneer, Korea) following the vendor's protocol. Thereafter, the degree of DNA damage was evaluated by electrophoresis using equal amounts of purified DNA on a 1% agarose gel, with undigested pUC19 vector DNA as a reference. The observed results were confirmed in triplicated assays.

2.6. Oxidative stress tolerance assay

In order to determine potential rRfCat-mediated resistance to oxidative stress in bacterial cells, *E. coli* strain BL21 (DE3) was transformed with the pMAL-c2X-*RfCat* recombinant vector or vector alone (control). Cells were grown in 10 mL LB medium supplemented with ampicillin (100 µg/mL) and glucose (0.2%) until an optical density (OD) of 0.6 at 600 nm was reached. Subsequently, the cultures were induced by IPTG (0.5 mM) to overexpress the corresponding proteins (rRfCat or MBP), and further incubated at 20 °C for 9 h with shaking. Thereafter, 1 mL of each culture (~1 × 10⁶ CFU/mL) was spun down, and the cell pellets were resuspended in fresh LB medium (1 mL), supplemented with ampicillin (100 µg/mL), glucose (0.2%), and IPTG (0.5 mM), with or without the addition of H₂O₂ (500 µM). Thereafter, the cultures were incubated 20 °C overnight with shaking. The following day the cultures were serially diluted with sterile phosphate buffered saline (1%), plated (100 µL) on ampicillin (100 µg/mL)/agar and incubated at 37 °C for 16 h. The number of colony forming units in each 1 mL culture was determined by counting the colonies on the corresponding plates in triplicates.

2.7. Fish rearing and tissue collection

Healthy fish acclimatized to the laboratory conditions were obtained from the aquariums at the Marine Science Institute of Jeju National University, Jeju Self Governing Province, Republic of Korea, and were maintained in 400 L laboratory aquarium tanks filled with aerated seawater at 22 ± 1 °C. Five healthy fish with an average body weight of 200 g were sacrificed for the tissue collection. Before sacrifice, approximately 1 mL blood was collected from each fish using sterile syringes coated with 0.2% heparin sodium salt (USB, USA), and the peripheral blood cells were separated by immediate centrifugation at 3000 × g for 10 min at 4 °C. Other tissues including the head kidneys, spleen, liver, gills, intestines, kidney, brain, muscle, skin, heart, and stomach were excised and snap-frozen in liquid nitrogen and stored at –80 °C.

2.8. Immune challenge experiment

In order to analyze the transcriptional modulation of RfCat upon viral or bacterial stimulation, healthy rockfish with an average body weight of 200 g were used in a time course immune challenge experiment. The gram positive live bacterial pathogen *S. iniae* (10⁵ CFU/µL) and poly I:C (150 µg/µL; Sigma, St. Louis, MO, USA),

which resembles the double stranded viral RNA, were used as immune stimulants after re-suspending or dissolving in PBS. Fish were intraperitoneally injected with each stimulant in a total volume of 200 μ L. For the control group, fish were injected with 200 μ L PBS. Spleen tissues and blood were sampled from five individuals in each group at 3, 6, 12, 24, 48, and 72 h post-injection, as described in Section 2.7.

2.9. RNA extraction and cDNA synthesis

Total RNA was extracted from a pool of tissue samples (~40 mg from each fish) from five individual fish (both un-injected and injected) using QIAzol[®] (Qiagen), following the vendor's protocol. RNA samples purified from liver of healthy fish were further purified using RNeasy Mini Kit (Qiagen). RNA quality was examined by 1.5% agarose gel electrophoresis, and the concentration was determined at 260 nm in μ Drop Plate (Thermo Scientific). First strand cDNA was synthesized in a 20 μ L reaction mixture containing 2.5 μ g of RNA with the PrimeScript[™] II 1st strand cDNA Synthesis Kit (TaKaRa). The synthesized cDNA was diluted 40-fold in nuclease free water and stored in a freezer at -80°C until future use.

2.10. RfCat expression analysis by quantitative real time PCR (qPCR)

In order to analyze the basal expression levels of *RfCat* in the aforementioned tissues (Section 2.8) of healthy fish and to monitor transcriptional modulation in the blood cells and spleen of immune challenged animals in response to the corresponding immune stimulations, qPCR was applied using the respective diluted cDNA samples as templates (Section 2.9). qPCR was performed using the Dice[™] Real time system thermal cycler (TP800; TaKaRa, Japan) in a 10 μ L reaction volume, containing 3 μ L of diluted cDNA from each tissue, 5 μ L of 2 \times TaKaRa ExTaq[™] SYBR premix, 0.4 μ L of each primer (*RfCat*-qF and *RfCat*-qR; Table 1), and 1.2 μ L of ddH₂O, as per the essential MIQE guidelines [45]. PCR conditions were as follows: 95 $^{\circ}\text{C}$ for 10 s; 35 cycles of 95 $^{\circ}\text{C}$ for 5 s, 58 $^{\circ}\text{C}$ for 10 s, and 72 $^{\circ}\text{C}$ for 20 s; and a final cycle of 95 $^{\circ}\text{C}$ for 15 s, 60 $^{\circ}\text{C}$ for 30 s, and 95 $^{\circ}\text{C}$ for 15 s. Each assay was conducted in triplicates. The baseline was set automatically by the Dice[™] Real Time System software (version 2.00). The relative *RfCat* expression was determined using the Livak ($2^{-\Delta\Delta\text{CT}}$) method [46]. The black rockfish elongation factor 1 α (*RfEF1A*) gene was used as an internal reference (GenBank ID: KF430623), because it was previously validated as an appropriate internal control for qPCR normalization in black rockfish [47] gene expression studies. The primers used for the internal reference are listed in Table 1. The data are presented as the mean \pm standard deviation (SD) of the relative mRNA expression from three experiments. In the immune challenge experiments, the expression levels of *RfCat* mRNA were calculated relative to that of *RfEF1A*. The expression values were further normalized to the corresponding PBS-injected controls at each time point. The relative expression level in the un-injected control at 0 h was used as the baseline reference. To determine the statistical significance ($p < 0.05$) between the experimental and un-injected control groups, a two-tailed un-paired Student's *t*-test was applied.

3. Results and discussion

3.1. Sequence profiles, homology and phylogenetic relationship

Analysis of the black rockfish cDNA sequence database using the NCBI-BLASTX tool led to the identification of a 4337 bp contig sequence that was homologous to vertebrate catalases. The cDNA sequence of *RfCat* consisted of a 1581 bp coding region for a protein of 527 amino acids with a predicted molecular weight of

60 kD and a theoretical isoelectric point of 6.6, along with a 69 bp 5' un-translated region (5' UTR) and a 2687 bp 3' UTR. These sequence data were deposited in the NCBI-GenBank sequence database under the accession number KM401562. According to the *in silico* analysis of the protein sequence, *RfCat* contained the typical characteristic domain signatures of catalases, including a catalase proximal active site signature (residues 64–80, Fig. 1) and a catalase proximal heme ligand signature (residues 354–362). Moreover, our multiple sequence alignment study asserts that most of the heme binding sites and NADPH binding sites found in its homologues are also conserved in *RfCat* (Fig. 1), along with aforementioned signatures. As expected, *RfCat* shares prominent sequence similarity and identity with its fish counterparts, as per our pairwise sequence alignment. Black rockfish *RfCat* shared 88.8% identity and 94.5% similarity to rock bream (*O. fasciatus*) catalase (Table 2). However, *RfCat* also shows substantial sequence compatibility with mammals, amphibians, and invertebrates, such as insects and mollusks. Collectively, these data suggest high homology of *RfCat* with catalases from other species, further supporting its functional similarity with its homologues.

As expected, phylogenetic reconstruction, generated to evaluate the evolutionary position of *RfCat* among its homologues resulted in two independent clusters harboring vertebrates and invertebrates, forming an out group with yeast catalase (Fig. 2). Within the vertebrate clade, *RfCat* was clustered with its teleostan similitudes, with a closer evolutionary relationship with rock bream catalase, validated by a satisfactory bootstrap support (65). This further reinforces the similarity between the two species. In addition, within the fish sub-cluster, catalases of marine fish origin were distinctly clustered with those of fresh water fish origin, suggesting a relatively distant evolutionary relationship between these groups. Moreover, insect catalases maintain a notable evolutionary proximity to vertebrate catalases, as compared to mollusks, forming a separate group diverging directly from the vertebrate cluster (Fig. 2). Overall, this phylogenetic analysis confirms the common vertebrate ancestral origin of *RfCat*, further validating its homology with teleost catalases.

3.2. Tertiary structural model of RfCat

In order to anticipate the putative relationship between the folded structural arrangement and functional properties of *RfCat*, we generated a model of its tertiary structure using an 'iterative template fragment assembly simulation' method by I-TASSER online server and visualized by the PyMOL 1.7 program. According to the modeling results, the whole template chains of the top ten templates obtained from the Research Collaboratory for Structural Bioinformatics protein data bank (RCSB-PDB) shared over 90% sequence identity with the query sequence. Importantly, the normalized Z-score of the threading alignments between each template sequence and query sequence exceeded 1 (2.39–8.00), supporting the credibility of the model. Human erythrocyte catalase (RCSB-PDB ID: 1DGF) was used as the highest ranked template for the model generation by the server.

According to the predicted model (Fig. 3), four conceptual domains, the N-terminal domain forming an extended non-globular amino terminal arm, the C terminal domain with four prominent α helices, the β -barrel domain with eight stranded anti-parallel β -sheets, and the connection domain harboring a wrapping or folding loop, could be identified, supporting its homology to the empirically determined tertiary structure of human catalase [17]. Moreover, the proximal active site motif could be identified at the middle of our modeled structure, close to the β -barrel domain, and was exposed to the external environment, which may be a favorable

orientation for access its substrates. Collectively, the generated model of RfCat could plausibly validate its structural arrangement for the anticipated catalytic function.

3.3. Integrity and purity of overexpressed rRfCat

Analysis of samples collected at different steps of the purification process using SDS-PAGE confirmed the expression of rRfCat after IPTG induction under the given experimental conditions (Fig. 4). However, the eluted sample of the purified fusion rRfCat resolved two bands on the gel (Fig. 4; lane 3), one of which (~102.5 kD) matched the predicted size of RfCat (60 kD), since the molecular mass of MBP is ~42.5 kD. The other band appears below the expected size of the fusion protein, possibly due to self-cleavage of the rRfCat, as vertebrate catalases can be epigenetically modified by processes including proteolysis, in turn resulting in truncated forms of the original enzyme [48,49]. Moreover, this type of degradation is frequently observed in recombinantly expressed catalases, even with invertebrate origins, such as disk abalones, as reported previously [50].

3.4. Peroxidase activity

The peroxidase activity of RfCat was investigated using its purified recombinant protein as a function of the enzyme or substrate (H₂O₂) concentration. As plotted in Fig. 5A, increasing the RfCat concentration dose-dependently increased its relative activity. The relative peroxidase activity of rRfCat reached a maximum value when 54 µg/mL protein was used in the reaction, and the activity maintained almost a constant value with further increases in concentration, suggesting this was the optimal activity level for this protein. As expected, MBP did not show any detectable activity at any concentration, supporting that the effects were due to the rRfCat portion in the rRfCat recombinant fusion protein. Intriguingly, a similar pattern of peroxidase activity was detected with increasing concentrations of rock bream catalase, reported in our previous study [31]. In contrast, with the increasing concentration of the H₂O₂, the relative activity of rRfCat tends to gradually decrease. However, the maximum concentration of the H₂O₂ (11.2 mM) used in the assay was almost 11 fold higher than the minimum. Nevertheless, rRfCat could still demonstrate ~70% of its

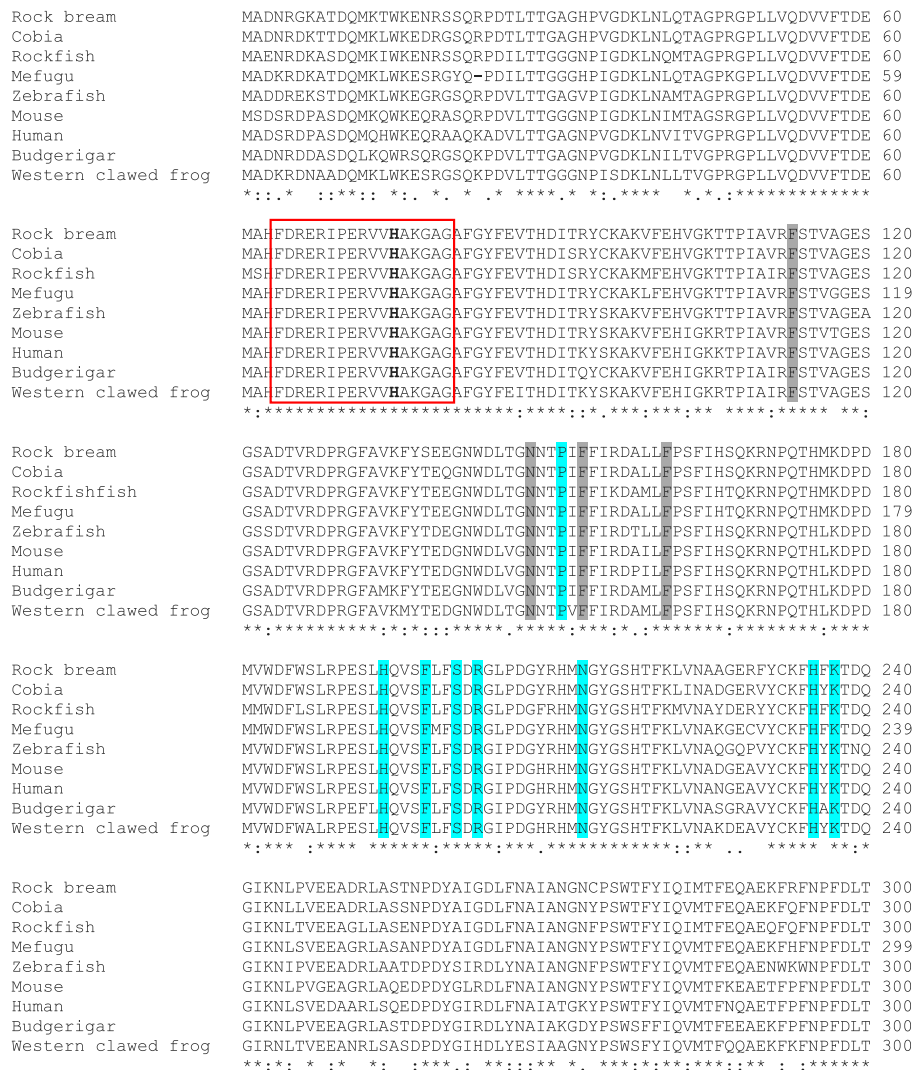


Fig. 1. Multiple sequence alignment of vertebrate catalases, including black rockfish catalase (RfCat). The proximal heme ligand signature was denoted by red colored boxes bordered by continuous or non-continuous lines, respectively. Conserved heme binding sites and NADPH binding sites were indicated by gray color and blue color shading, respectively. Residues conserved in all the aligned sequences are represented by asterisks (*) whereas partially conserved ones were marked using (·) or (:). (For interpretation of the references to color in this figure legend, the reader is referred to the web version of this article.)

Rock bream	KIWSHKEYPLIPVGMVLRNRPVNYFAEVEQLAFDPSNMPPGIEFSPDKMLQQRLEFSYPD	360
Cobia	KVWSHKEYPLIPVGRMVLNRNRPVNYFAEVEQLAFDPSNMPPGIEFSPDKMLQQRLEFSYPD	360
Rockfish	KIWPQKEYPLIPVGLVLRNRPVNYFAEVEQLAFDPSNMPPGIEFSPDKMLQQRLEFSYPD	360
Mefugu	KVWSHKEYPLIPVGMVLRNRPVNYFAEVEQMAHDPNSMPPGIEFSPDKMLQQRLEFSYPD	359
Zebrafish	KVWSHKEYPLIPVGRFVLRNRPVNYFAEVEQLAFDPSNMPPGIEFSPDKMLQQRLEFSYPD	360
Mouse	KVWPBKDYPLIPVGLVLRNRPVNYFAEVEQMAFDPNSMPPGIEFSPDKMLQQRLEFSYPD	360
Human	KVWPBKDYPLIPVGLVLRNRPVNYFAEVEQIAFDPSNMPPGIEASPDKMLQQRLEFSYPD	360
Budgerigar	KIWPBGDYPLIPVGLVLRNRPVNYFAEVEQMAFDPNSMPPGIEFSPDKMLQQRLEFSYPD	360
Western clawed frog	KIWPBGDYPLIPVGLVLRNRPVNYFAEVEQLAFDPSNMPPGIEFSPDKMLQQRLEFSYPD	360
	*.:. :.:*****:***:*.*.***:****:*.***** **.******:***:***	
Rock bream	THRHRLGANYLQIPVNCPPFRARVNTYQRDGPMSMFDNQGGAPNYYPNSFSAPETQPQFVE	420
Cobia	THRHRLGANYLQIPVNCPPFRARVANYQRDGPMSMFDNQGGAPNYYPNSFSAPETQPQFME	420
Rockfish	THRHRLGANYLQIPVNCPPFRARVNSYRRDGPMSMFDNQGGAPNYYPNSFSAPETQPRFVE	420
Mefugu	THRHRLGANYLQIPVNCPPYRTRVANYQRDGPMSMFDNQGGAPNYYPNSFSAPETQPQFVE	419
Zebrafish	THRHRLGANYLQIPVNCPPYRTRVANYQRDGPMSMFDNQGGAPNYYPNSFSAPDVQPRFLE	420
Mouse	THRHRLGPNYLQIPVNCPPYRARVANYQRDGPMSMFDNQGGAPNYYPNSFSAPETQPRFVE	420
Human	THRHRLGPNYLQIPVNCPPYRARVANYQRDGPMSMFDNQGGAPNYYPNSFGAPEQPQSALE	420
Budgerigar	THRHRLGPNYLQIPVNCPPFRTRVANYQRDGPMSMFDNQGGAPNYYPNSFTGPEQPQVWRE	420
Western clawed frog	THRHRLGPNYLQIPVNCPPYRTRVANYQRDGPMSMFDNQGGAPNYYPNSFCAPENQPVQRE	420
	*.:. :.:*****:***:*.*.***:****:*.***** **.******:***:***	
Rock bream	SKFKVSPDVARYNSADEDNVTQVRTFYTVLNEEERQRLCQNMAGALKGAQLFIQKRMVE	480
Cobia	SKFKVSPDVGRYNSADEDNVTQVRAFVTVLNEEERQRLCQNLGALKGAQLFIQKRMVE	480
Rockfish	SKFKVSPDVARYNTDDEDNVTQVCNFMVRLNEEERQRLCQNLGALKGAQLFIQKRMVE	480
Mefugu	SKFKVYPDVARYNSSDEDNVTQVRTFYAEVLDNEEERQRLCENFAGSLKGAQLFIQKRMVE	479
Zebrafish	SKKCVSPDVARYNSADDDNVTQVRTFFTVLNEEERQRLCQNMAGHLKGAQLFIQKRMVE	480
Mouse	HSVQCAVDVRFNSANEDNVTQVRTFYTVLNEEERKRLCENIAGHLKDAQLFIQKRAVK	480
Human	HSIQYSGEVRFRNTANDDNVTQVRAFVTVLNEEERKRLCENIAGHLKDAQLFIQKRAVK	480
Budgerigar	SRMSISGDVQRFNSANEDNVTQVRDFYTVLKEDEERQRLCENIADHLKDAQLFIQKRAVK	480
Western clawed frog	HRFHVSADVARYNSADEDNVSQVRDFYVVKVLSSEERQRLCENIAGHLKDAQLFIQKRAVK	480
	*.:. :.:*****:***:*.*.***:****:*.***** **.******:***:***	
Rock bream	NLKAHPDYGNRVQTLNKNYNAEAQKNTTVHVYSRPGASAVAAASSKM-	527
Cobia	NLKAHPDYGNRVQTLNKNYNAEAHKSSTVVRYSRPGASAVAAASSKM-	527
Rockfish	TLNAVHPDYGSRVQTLNKNYNAEAQKNTTVHVYSRPGTSAIAASSKM-	527
Mefugu	NLKAHPDYASRVQKFLDKYNEEAENAHVRYTRPGASAVAAASSKM-	526
Zebrafish	NLMAVHSDYGNRVQALLDKHNAEGKKN-TVHVYSRGGASAVAAASSKM-	526
Mouse	NFTDVHPDYGARIQALLDKYNAEK-PKNAIHTYVQAGSHMAAKGKANL	527
Human	NFTDVHPDYGSHIALLDKYNAEK-PKNAIHTYVQAGSHMAAREKANL	527
Budgerigar	NFTDVHPDYGARIQALLDKYNADSGKDVIRTYTQSTSRMSAKERSNL	528
Western clawed frog	NFTDVHPDYGARIQALLDKYNAEGAKKTKVKTQSTYATADKANL	528
	.. :.:*****:***:*.*.***:****:*.***** **.******:***:***	

Fig. 1. (continued).

relative peroxidase activity, only losing ~15% of its relative activity compared to its minimal substrate concentration (~85%). This observation suggests that rRfCat can withstand substantial levels of oxidative stress mounted by H₂O₂.

3.5. Oxidative DNA damage protection activity

The protective effect of rRfCat against ROS-induced DNA damage by a Fenton type reaction [51] was evaluated by MFO assay using

plasmid DNA. As depicted in Fig. 6, in the presence of rRfCat, the conversion of pUC19 plasmid DNA from supercoiled to nicked form was inhibited (Fig. 6; lane 4). However, in the absence of rRfCat or presence of MBP, supercoiled plasmid DNA was significantly nicked, as evidenced by intense bands observed corresponding to the nicked form of DNA (lanes 2 and 3). These observations indicate that hydroxyl radicals formed by the reaction system can damage DNA, and those can be scavenged by rRfCat, likely through its peroxidase activity. Importantly, the involvement of the MBP in the

Table 2
Percentage similarity and identity values of RfCat with homologues.

Species	Common name	Taxonomy	GenBank accession number	Length in amino acids	Identity%	Similarity%
1. <i>Oplegnathus fasciatus</i>	Rock bream	Fish	AAU44617	527	88.8	94.5
2. <i>Rachycentron canadum</i>	Cobia	Fish	ACO07305	527	86.3	93.5
3. <i>Takifugu obscurus</i>	Mefugu	Fish	ABV24056	526	85	91.8
4. <i>Kryptolebias marmoratus</i>	Mangrove rivulus	Fish	ABW88893	527	83.9	91.1
5. <i>Hypophthalmichthys nobilis</i>	Bighead carp	Fish	ADK27719	525	81.8	91.8
6. <i>Danio rerio</i>	Zebrafish	Fish	NP_570987	526	80.8	91.7
7. <i>Mus musculus</i>	Mouse	Mammalia	NP_033934	527	78.1	87.7
8. <i>Canis lupus familiaris</i>	Dog	Mammalia	BAB20764	527	77.9	88.5
9. <i>Bos taurus</i>	Cattle	Mammalia	NP_001030463	527	77.3	87.5
10. <i>Xenopus tropicalis</i>	Western clawed frog	Amphibia	NP_001072167	528	77.1	88.1
11. <i>Xenopus laevis</i>	African clawed frog	Amphibia	NP_001080544	528	75.8	85
12. <i>Melopsittacus undulatus</i>	Budgerigar	Aves	AAO27213	528	75.8	87.1
13. <i>Homo sapiens</i>	Human	Mammalia	NP_001743	527	75.6	86.2
14. <i>Columba livia</i>	Rock pigeon	Aves	EMC81385	514	73.3	83.9
15. <i>Azumapecten farreri</i>	Scallop	Mollusca	ABI64115	507	65.5	78.9
16. <i>Drosophila melanogaster</i>	Fruit fly	Insecta	NP_536731	506	62.6	75.5
17. <i>Haliotis discus discus</i>	Disc abalone	Mollusca	ABQ60044	501	62.4	76.1
18. <i>Aedes aegypti</i>	Mosquito	Insecta	XP_001663600	505	61.2	73.6
19. <i>Bombyx mori</i>	Silkworm	Insecta	NP_001036912	507	60.8	73.5
20. <i>Saccharomyces cerevisiae</i>	Yeast	fungi	NP_010542	515	45.3	58.2
21. <i>Gallus gallus</i>	Chicken	Aves	NP_001026386	235	36.8	40.2

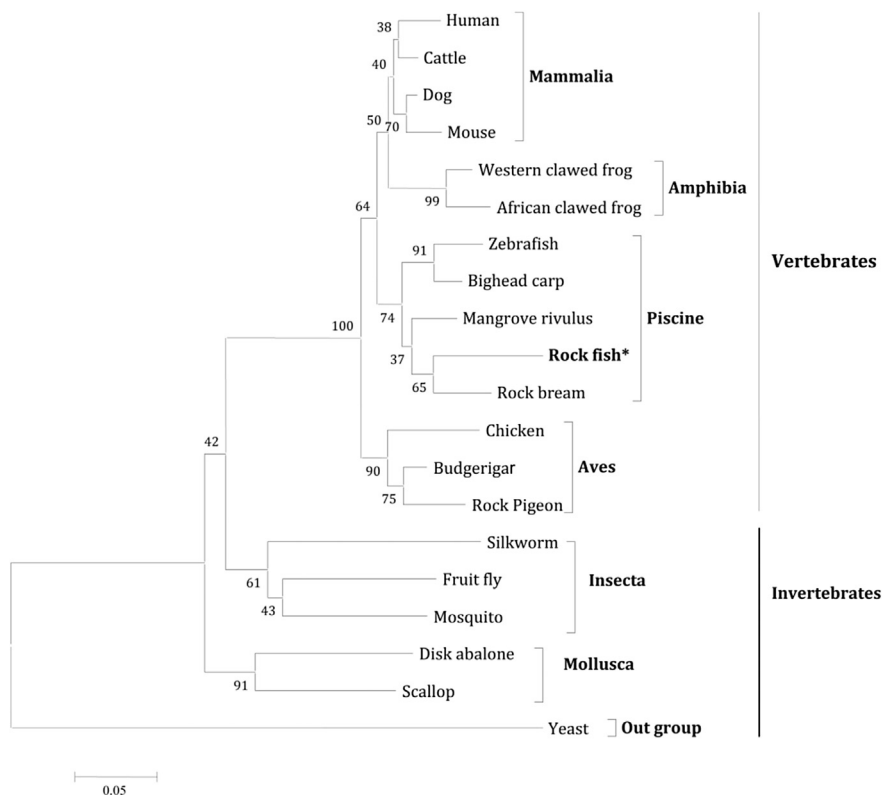


Fig. 2. Phylogenetic reconstruction of RfCat, generated based on the ClustalW multiple sequence alignment of vertebrate and invertebrate catalase homologues, evaluated by the neighbor-joining method using MEGA version 4.0. Bootstrap supporting values are noted in the corresponding branches and NCBI-GenBank accession numbers of each homolog were mentioned in Table 2.

fusion protein was negligible. These observations affirm the clear role of RfCat in ROS scavenging, thereby preventing oxidative DNA damage.

3.6. Tolerance of oxidative stress

Overexpressing rRfCat in *E. coli* (DE3) cells, we investigated the potential RfCat-induced resistance to H₂O₂-mediated oxidative

damage in bacterial cells. To determine the survival of *E. coli* under H₂O₂ stress, the cells were transformed with a pMAL-RfCat fusion construct. These cells exhibited a significantly higher level ($p < 0.05$) of survival (6×10^{10} CFU/mL) than the cells transformed with only the pMAL-c2X vector (1.2×10^{10} CFU/mL) (Fig. 7), indicating that rRfCat overexpressing cells were more resistant to H₂O₂-mediated oxidative damage on *E. coli*. Moreover, it further

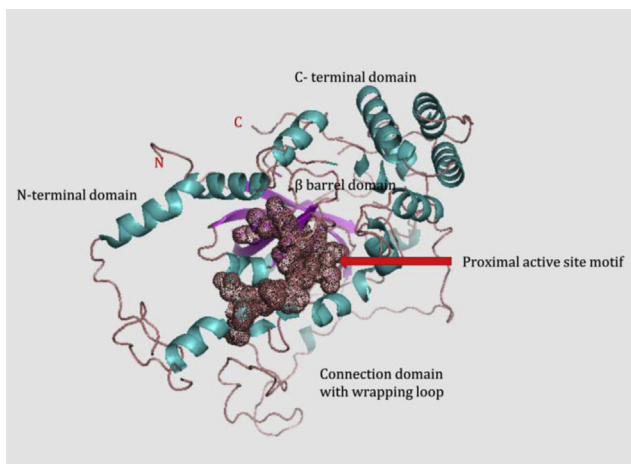


Fig. 3. Tertiary structural model of RfCat generated by I-TASSER server. α -Helices and β -sheets are indicated by green and pink color, respectively. Four conceptual domains were denoted in the model. Residues forming the proximal active site signature were depicted at the middle of the model in the brown color, using spherical bulges. Amino and carboxyl terminals of the protein were indicated by N and C letters, respectively. (For interpretation of the references to color in this figure legend, the reader is referred to the web version of this article.)

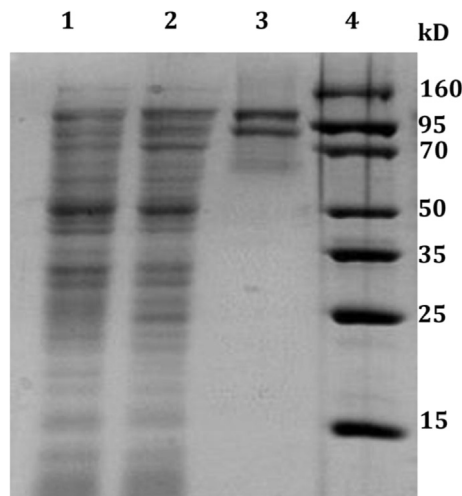


Fig. 4. SDS-PAGE analysis of purified recombinant RfCat (rRfCat) fusion protein with the samples collected at different steps of the rRfCat purification. Lane 1, Total soluble cellular extract from *E. coli* BL21 (DE3) harboring the rRfCat-MBP fusion vector construct prior to IPTG induction; lane 2, Crude extract of rRfCat after IPTG induction; lane 3, Purified rRfCat 4, Protein size marker (Enzymomics-Korea).

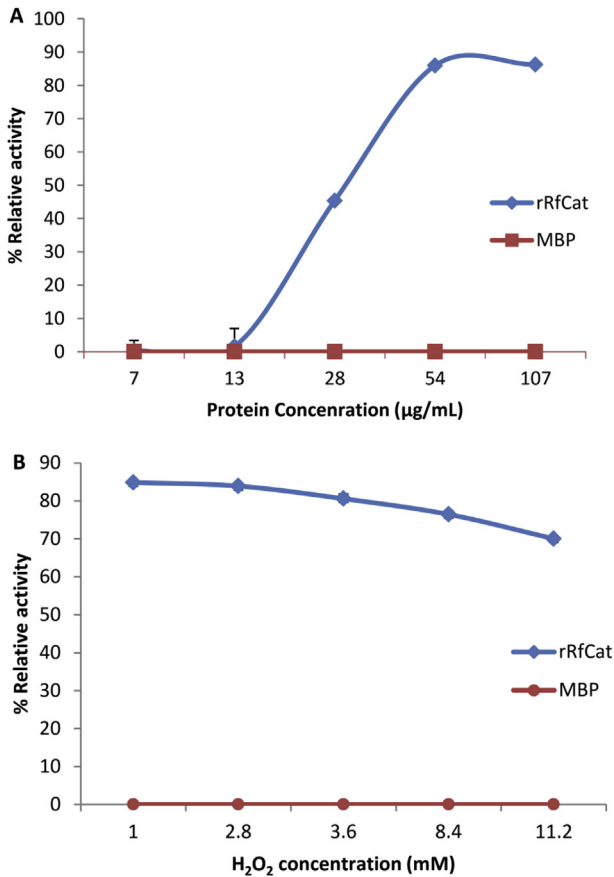


Fig. 5. *In vitro* peroxidase activity of rRfCat fusion protein against the substrate hydrogen peroxide A) at different concentrations of protein B) at different concentrations of substrate. Error bars represent the SD (n = 3).

suggests that MBP expressed in *E. coli* has no effect on oxidative stress tolerance. As expected, there was no significant difference observed between the recombinant bacterial cell growth under non-stress (without H₂O₂) conditions (data not shown). The resistance of rRfCat overexpressing *E. coli* to oxidative stress supports the notion that the peroxidase activity of rRfCat renders an oxidative damage protection. Collectively, these results indicate that RfCat can act as a potent antioxidant in a cellular environment under oxidative stress to protect the living cells from oxidative damage.

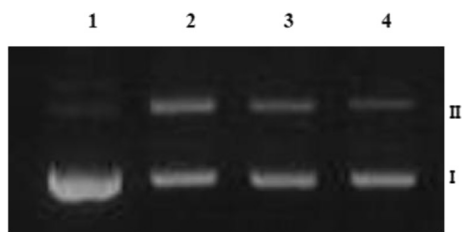


Fig. 6. Oxidative DNA damage protection activity of rRfCat, detected against ROS generated by MFO assay. After the MFO assay was performed with or without rRfCat or MBP, pUC19 plasmid DNA in each reaction mixture were analyzed by gel electrophoresis after a purification process, using 1% agarose gels. Lane 1, Undigested pUC19 plasmid DNA; lane 2, purified pUC19 in the reaction mixture without any treatment; lane 3, purified pUC19 in the reaction mixture treated with MBP (10 µg); and lane 4, purified pUC19 in the reaction mixture treated with rRfCat (10 µg). I – Supercoiled form of DNA; II – Nicked form of DNA.

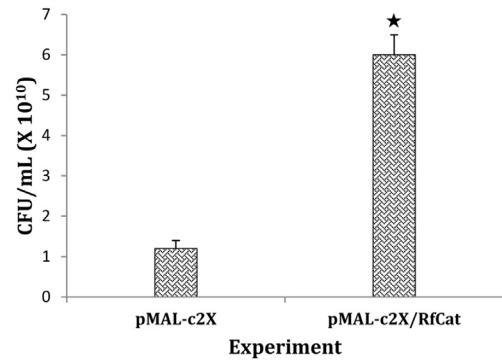


Fig. 7. Survival of *E. coli* BL21 (DE3) cells carrying pMAL-c2X or pMAL-c2X-RfCat recombinant vectors against H₂O₂-induced oxidative stress. The surviving bacterial count is presented as CFU in 1 mL of culture. Error bars represent the SD (n = 3); *p < 0.05.

3.7. Tissue specific mRNA expression of RfCat

According to the qPCR assay, *RfCat* mRNA was ubiquitously expressed in the tissues examined, albeit with widely different magnitudes (Fig. 8). The most pronounced basal expression of *RfCat* was found in the blood and liver, which is not unlike with the detected basal transcriptional profile of rock bream catalase in our previous study [31]. However, the fold difference between these two tissues was ~14. The difference in basal *RfCat* expression may reflect the proportionally variable levels of metabolic activity, which generates ROS under physiological conditions. Blood cells, especially phagocytes, play a key role in the elimination of foreign invaders, such as bacteria and parasites, or dead host cells, thereby consuming high levels of oxygen to form ROS [52]. Furthermore, there is higher ROS generating potential in blood cells induced by inflammatory cytokines produced by immune cells, including macrophages, B lymphocytes, T lymphocytes, and mast cells under septic conditions [53]. Therefore, maintaining a strong antioxidant system in blood, including endogenous antioxidants such as catalase is necessary to counterbalance the overproduction of ROS in these cells. The liver is also considered an organ that regulates the high metabolic rate, and in turn, its cells can undergo oxidative stress due to excessive production of ROS, leading to cellular apoptosis [54]. Thus, it is not surprising to observe substantial

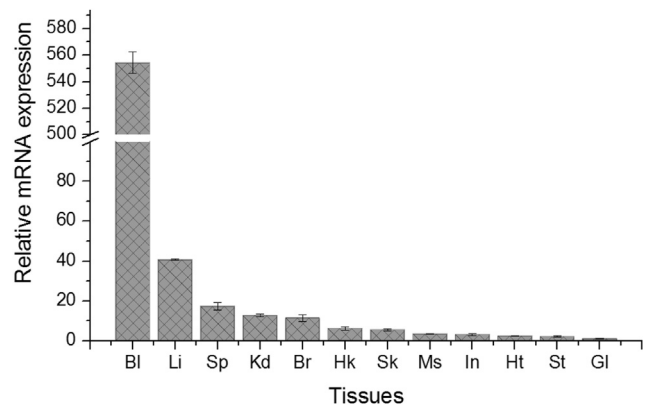


Fig. 8. Tissue-specific distribution of *RfCat* expression in black rockfish measured using quantitative real-time polymerase chain reaction (qPCR). Fold-change in expression is shown relative to the mRNA expression level in gill tissue. Error bars represent SD (n = 3). Bl – Blood; Li – Liver; Sp – Spleen; Kd – Kidney; Br – Brain; Hk – Head kidney; Sk – Skin; Ms – Muscle; In – Intestine; Ht – Heart; St – Stomach; Gl – Gill.

expression of *RfCat* in liver cells. Similar to our observation, mefugu (*Takifugu obscurus*) catalase was abundantly detected in liver tissue [55], whereas the catalase of zebrafish was prominently detected in its abdominal section [32].

3.8. Transient transcriptional modulation of *RfCat* under pathogen stress

In order to evaluate the role of *RfCat* in redox homeostasis mediated by dismutation of peroxides formed upon pathogen invasion, its temporal transcriptional modulation was determined under pathogenic stress in blood and spleen tissues, which are known to regulate the first line host defense mechanisms [56]. Herein, we used *S. iniae* as the live pathogenic bacterial stimulant, since it is one of the common and serious aquatic pathogens causes deadly infectious diseases in farmed marine finfish species [57]. In blood tissue, the invasion of the pathogenic bacteria *S. iniae* significantly ($p < 0.05$) enhanced the basal transcript level of *RfCat* during the middle phase (12 h) post-stimulation (p.s.), while significantly ($p < 0.05$) diminishing the expression at late phases (72 h) p.i. (Fig. 9A). Similarly, upon stimulation with the viral double stranded RNA emulator; poly I:C, basal expression of *RfCat* was significantly elevated and downregulated, but at late phases (24 h and 72 h, respectively) p.i. (Fig. 9A). Collectively, bacterial or viral stimulants could only trigger late transcriptional responses in blood, with a lesser fold difference compared to the basal level of *RfCat* expression (0 h). This observation can be plausibly explained

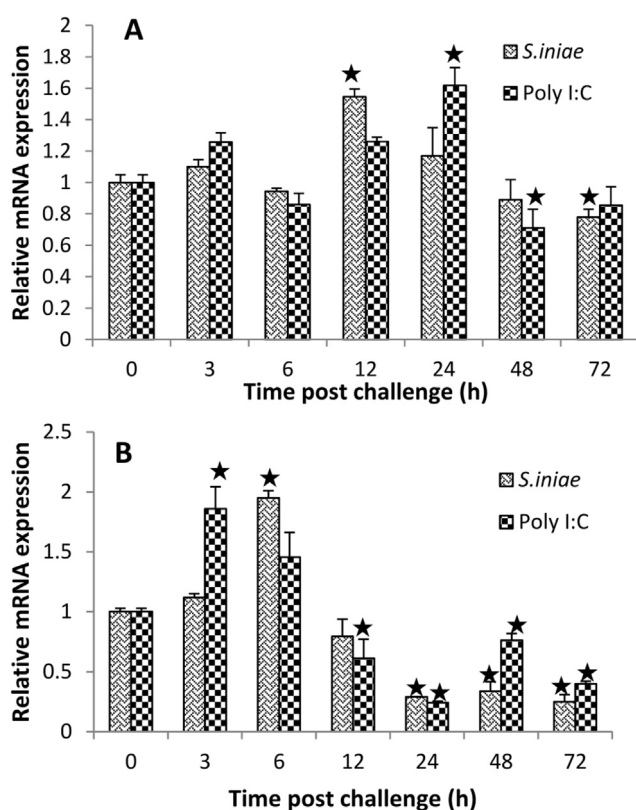


Fig. 9. Temporal modulation of *RfCat* transcription in A) blood cells and B) spleen tissues upon immune stimulation with poly I:C and *S. iniae*, as determined using qPCR. The relative expression was calculated using the $2^{-\Delta\Delta CT}$ method. The black rockfish EF1A gene was used as the reference gene and expression was further normalized to that of corresponding PBS-injected controls at each time point. The relative fold-change in expression at 0 h post-injection was used as the baseline. Error bars represent SD (n = 3); * $p < 0.05$.

by the pronounced basal expression of *RfCat* in blood tissue, which may adequately withstand the oxidative stress that occurs upon identification of pathogens or pathogen associated molecular patterns (PAMPs) by the host defense system. Nevertheless, late phase downregulation of the *RfCat* transcriptional levels after both stimulations may reflect an mRNA turnover [58]. This may be a part of the counterbalancing process of antioxidant enzyme concentration against produced ROS concentration to maintain the ROS level at a steady state in cells. In our previous study, rock bream *catalase* was found to modulate the basal transcription under bacterial or viral stress in blood tissues, including bacterial (*E. tarda*) and poly I:C stimulation basal. mRNA expression was not significantly modulated at the early phase; but at middle phase p.s. (12 h) it was significantly induced nearly being compatible with our observation on *RfCat* transcript levels after *S. iniae* or poly I:C stimulation. Nevertheless, thereafter rock bream *catalase* mRNA returned to its basal level and maintained the same level throughout the experiment period.

In contrast, *S. iniae* and poly I:C significantly induced early phase transcription ($p < 0.05$) (6 h and 3 h p.i., respectively) in the spleen, although the transcriptional levels were decreased with fluctuations (Fig. 9B). As spleen is a potent organ in host immunity, ROS generation upon recognition of pathogens or PAMPs by the host immune system may rapidly occur. Hence, to counterbalance these ROS, *RfCat* expression may elevate in spleen cells, since its basal mRNA level is not sufficient compared to blood cells (Fig. 8). This, in turn prepares cells to tolerate oxidative stress. However, since catalases have a very limited distribution in cells and localized exclusively in peroxisomes, catalases may not be actively involved in ROS scavenging until ROS get reached to the peroxisomes. Instead, other antioxidant enzymes (glutathione peroxidases and thioredoxin peroxidases) which can easily access ROS including H_2O_2 and have higher affinity for them may be promptly involved in detoxification of over produced ROS [59,60]. Similar to what we have observed in blood, decreased but fluctuating transcriptional profile was observed with significant downregulation after the inductive response of *RfCat* transcription upon both stimuli in spleen. This observation may be a reflection of the aforementioned notion or may hint a regulatory mechanism functioning through balancing between the mRNA turnover and synthesis of antioxidants to maintain the redox balance in cells after increase of catalases like antioxidant enzymes. On the other hand, it may hint a detrimental effect on fish health under the pathogenic stress, especially regarding live bacterial infection, since lesser concentration of antioxidants in turn lead to elevate the ROS level in cellular environment. This can cause oxidative stress and ultimately the cell death [61].

4. Conclusion

In this study, a new teleostan catalase homolog was identified from black rockfish (*RfCat*), and its structure and function was molecularly characterized. According to the *in silico* study, *RfCat* resembled the typical domain signatures of known catalases, further sharing homology with them. Our phylogenetic reconstruction clearly supported the vertebrate ancestral origin of *RfCat*, further reinforcing its homology with fish counterparts. Recombinantly expressed *RfCat* demonstrated prominent peroxidase activity with varying substrate and *RfCat* concentrations, detectable in the bacterial cell and the DNA protection activity assay. These functional insights clearly indicated a putative role of *RfCat* as an antioxidant. Additionally, *RfCat* in black rockfish was expressed in different tissues with varying magnitudes, indicating its importance in different tissues under physiological conditions. Moreover, basal transcription of *RfCat* was observed to be modulated by

immune stimulation, suggesting its potential involvement in maintaining the redox balance in cells under pathogenic stress.

Acknowledgments

This research was supported by the project titled 'Development of Fish Vaccines and Human Resource Training', funded by the Ministry of Oceans and Fisheries, Korea and by a grant from Marine Biotechnology Program (PJT200620, Genome Analysis of Marine Organisms and Development of Functional Applications) funded by Ministry of Oceans and Fisheries, Korea.

References

- [1] Eckersall PD, Bell R. Acute phase proteins: biomarkers of infection and inflammation in veterinary medicine. *Vet J* 2010;185:23–7.
- [2] Leto TL, Morand S, Hurt D, Ueyama T. Targeting and regulation of reactive oxygen species generation by Nox family NADPH oxidases. *Antioxid Redox Signal* 2009;11:2607–19.
- [3] Morey M, Serras F, Baguna J, Hafen E, Corominas M. Modulation of the Ras/ MAPK signalling pathway by the redox function of selenoproteins in *Drosophila melanogaster*. *Dev Biol* 2001;238:145–56.
- [4] Nakano H, Nakajima A, Sakon-Komazawa S, Piao JH, Xue X, Okumura K. Reactive oxygen species mediate crosstalk between NF-kappaB and JNK. *Cell Death Differ* 2006;13:730–7.
- [5] Buonocore G, Perrone S, Tataranno ML. Oxygen toxicity: chemistry and biology of reactive oxygen species. *Semin Fetal Neonatal Med* 2010;15: 186–90.
- [6] Circu ML, Aw TY. Reactive oxygen species, cellular redox systems, and apoptosis. *Free Radic Biol Med* 2010;48:749–62.
- [7] Kowaltowski AJ, de Souza-Pinto NC, Castilho RF, Vercesi AE. Mitochondria and reactive oxygen species. *Free Radic Biol Med* 2009;47:333–43.
- [8] Wang C, Yue X, Lu X, Liu B. The role of catalase in the immune response to oxidative stress and pathogen challenge in the clam *Meretrix meretrix*. *Fish Shellfish Immunol* 2013;34:91–9.
- [9] Nordberg J, Arner ES. Reactive oxygen species, antioxidants, and the mammalian thioredoxin system. *Free Radic Biol Med* 2001;31:1287–312.
- [10] Abele D, Puntarulo S. Formation of reactive species and induction of antioxidant defence systems in polar and temperate marine invertebrates and fish. *Comp Biochem Physiol A Mol Integr Physiol* 2004;138:405–15.
- [11] Nicholls P. Classical catalase: ancient and modern. *Arch Biochem Biophys* 2012;525:95–101.
- [12] Oshino N, Chance B, Sies H, Bucher T. The role of H₂O₂ generation in perfused rat liver and the reaction of catalase compound I and hydrogen donors. *Arch Biochem Biophys* 1973;154:117–31.
- [13] Nicholls P, Fita I, Loewen PC. Enzymology and structure of catalases. *Adv Inorg Chem* 2000;51:51–106.
- [14] Kashiwagi A, Kashiwagi K, Takase M, Hanada H, Nakamura M. Comparison of catalase in diploid and haploid *Rana rugosa* using heat and chemical inactivation techniques. *Comp Biochem Physiol B Biochem Mol Biol* 1997;118: 499–503.
- [15] Klotz MG, Klassen GR, Loewen PC. Phylogenetic relationships among prokaryotic and eukaryotic catalases. *Mol Biol Evol* 1997;14:951–8.
- [16] Yamamoto K, Banno Y, Fujii H, Miake F, Kashige N, Aso Y. Catalase from the silkworm, *Bombyx mori*: gene sequence, distribution, and overexpression. *Insect Biochem Mol Biol* 2005;35:277–83.
- [17] Putnam CD, Arvai AS, Bourne Y, Tainer JA. Active and inhibited human catalase structures: ligand and NADPH binding and catalytic mechanism. *J Mol Biol* 2000;296:295–309.
- [18] Mackay WJ, Bewley GC. The genetics of catalase in *Drosophila melanogaster*: isolation and characterization of acatalasemic mutants. *Genetics* 1989;122: 643–52.
- [19] Bryant DD, Wilson GN. Differential evolution and expression of murine peroxisomal membrane protein genes. *Biochem Mol Med* 1995;55:22–30.
- [20] McClung CR. Regulation of catalases in Arabidopsis. *Free Radic Biol Med* 1997;23:489–96.
- [21] Storz G, Tartaglia LA. OxyR: a regulator of antioxidant genes. *J Nutr* 1992;122: 627–30.
- [22] Goyal MM, Basak A. Human catalase: looking for complete identity. *Protein Cell* 2010;1:888–97.
- [23] Vigneshkumar B, Pandian SK, Balamurugan K. Catalase activity and innate immune response of *Caenorhabditis elegans* against the heavy metal toxin lead. *Environ Toxicol* 2013;28:313–21.
- [24] Ha EM, Oh CT, Ryu JH, Bae YS, Kang SW, Jang IH, et al. An antioxidant system required for host protection against gut infection in *Drosophila*. *Dev Cell* 2005;8:125–32.
- [25] Mohankumar K, Ramasamy P. White spot syndrome virus infection decreases the activity of antioxidant enzymes in *Fenneropenaeus indicus*. *Virus Res* 2006;115:69–75.
- [26] Zhang Q, Li F, Zhang X, Dong B, Zhang J, Xie Y, et al. cDNA cloning, characterization and expression analysis of the antioxidant enzyme gene, catalase, of Chinese shrimp *Fenneropenaeus chinensis*. *Fish Shellfish Immunol* 2008;24:584–91.
- [27] Mathew S, Kumar KA, Anandan R, Viswanathan Nair PG, Devadasan K. Changes in tissue defence system in white spot syndrome virus (WSSV) infected *Penaeus monodon*. *Comp Biochem Physiol C Toxicol Pharmacol* 2007;145:315–20.
- [28] Arockiaraj J, Easwwaran S, Vanaraja P, Singh A, Othman RY, Bhasu S. Molecular cloning, characterization and gene expression of an antioxidant enzyme catalase (MrCat) from *Macrobrachium rosenbergii*. *Fish Shellfish Immunol* 2012;32:670–82.
- [29] Li C, Ni D, Song L, Zhao J, Zhang H, Li L. Molecular cloning and characterization of a catalase gene from Zhikong scallop *Chlamys farreri*. *Fish Shellfish Immunol* 2008;24:26–34.
- [30] Guo H, Zhang D, Cui S, Chen M, Wu K, Li Y, et al. Molecular characterization and mRNA expression of catalase from pearl oyster *Pinctada fucata*. *Mar Genomics* 2011;4:245–51.
- [31] Elvitigala DA, Premachandra HK, Whang I, Priyathilaka TT, Kim E, Lim BS, et al. Marine teleost ortholog of catalase from rock bream (*Oplegnathus fasciatus*): molecular perspectives from genomic organization to enzymatic behavior with respect to its potent antioxidant properties. *Fish Shellfish Immunol* 2013;35:1086–96.
- [32] Gerhard GS, Kauffman EJ, Grundy MA. Molecular cloning and sequence analysis of the *Danio rerio* catalase gene. *Comp Biochem Physiol B Biochem Mol Biol* 2000;127:447–57.
- [33] Ken CF, Lin CT, Wu JL, Shaw JF. Cloning and expression of a cDNA coding for catalase from zebrafish (*Danio rerio*). *J Agric Food Chem* 2000;48:2092–6.
- [34] Nam YK, Cho YS, Choi BN, Kim KH, Kim SK, Kim DS. Alteration of antioxidant enzymes at the mRNA level during short-term starvation of rockbream *Oplegnathus fasciatus*. *Fish Sci* 2005;71:1385–7.
- [35] Tort L. Stress and immune modulation in fish. *Dev Comp Immunol* 2011;35: 1366–75.
- [36] Droeghe M, Hill B. The Genome Sequencer FLX System – longer reads, more applications, straight forward bioinformatics and more complete data sets. *J Biotechnol* 2008;136:3–10.
- [37] Campanella JJ, Bitincka L, Smalley J. MatGAT: an application that generates similarity/identity matrices using protein or DNA sequences. *BMC Bioinform* 2003;4:29.
- [38] Tamura K, Dudley J, Nei M, Kumar S. MEGA4: Molecular Evolutionary Genetics Analysis (MEGA) software version 4.0. *Mol Biol Evol* 2007;24:1596–9.
- [39] Zhang Y. I-TASSER server for protein 3D structure prediction. *BMC Bioinform* 2008;9:40.
- [40] Roy A, Kucukural A, Zhang Y. I-TASSER: a unified platform for automated protein structure and function prediction. *Nat Protoc* 2010;5:725–38.
- [41] Umasuthan N, Whang I, Kim JO, Oh MJ, Jung SJ, Choi CY, et al. Rock bream (*Oplegnathus fasciatus*) serpin, protease nexin-1: transcriptional analysis and characterization of its antiprotease and anticoagulant activities. *Dev Comp Immunol* 2011;35:785–98.
- [42] Bradford MM. A rapid and sensitive method for the quantitation of microgram quantities of protein utilizing the principle of protein-dye binding. *Anal Biochem* 1976;72:248–54.
- [43] Muller HE. Detection of hydrogen peroxide produced by microorganisms on an ABTS peroxidase medium. *Zentralbl Bakteriell Mikrob Hyg A* 1985;259: 151–4.
- [44] Kwon SJ, Kim K, Kim IH, Yoon IK, Park JW. Strand breaks in DNA induced by a thiol/Fe(III)/O₂ mixed-function oxidase system and its protection by a yeast antioxidant protein. *Biochem Biophys Res Commun* 1993;192:772–7.
- [45] Bustin SA, Benes V, Garson JA, Hellems J, Huggett J, Kubista M, et al. The MIQE guidelines: minimum information for publication of quantitative real-time PCR experiments. *Clin Chem* 2009;55:611–22.
- [46] Livak KJ, Schmittgen TD. Analysis of relative gene expression data using real-time quantitative PCR and the 2^{(-Delta Delta C(T))} method. *Methods* 2001;25:402–8.
- [47] Liman M, Wenji W, Conghui L, Haiyang Y, Zhigang W, Xubo W, et al. Selection of reference genes for reverse transcription quantitative real-time PCR normalization in black rockfish (*Sebastes schlegelii*). *Mar Genomics* 2013;11: 67–73.
- [48] Crane D, Holmes R, Masters C. Proteolytic modification of mouse liver catalase. *Biochem Biophys Res Commun* 1982;104:1567–72.
- [49] Sun Y. Multiplicity of antioxidant enzyme catalase in mouse liver cells. *Free Radic Res* 1997;26:343–50.
- [50] Ekanayake PM, De Zoysa M, Kang HS, Wan Q, Jee Y, Lee YH, et al. Cloning, characterization and tissue expression of disk abalone (*Haliotis discus discus*) catalase. *Fish Shellfish Immunol* 2008;24:267–78.
- [51] Crichton RR, Wilmet S, Leggsyer R, Ward RJ. Molecular and cellular mechanisms of iron homeostasis and toxicity in mammalian cells. *J Inorg Biochem* 2002;91:9–18.
- [52] Ernst JD, Stendahl O. Phagocytosis of bacteria and bacterial pathogenicity. New York Cambridge University Press; 2006.
- [53] Rezende-Oliveira K, Sarmento RR, Rodrigues Jr V. Production of cytokine and chemokines by human mononuclear cells and whole blood cells after infection with *Trypanosoma cruzi*. *Rev Soc Bras Med Trop* 2012;45:45–50.
- [54] Kamata H, Honda S, Maeda S, Chang L, Hirata H, Karin M. Reactive oxygen species promote TNFalpha-induced death and sustained JNK activation by inhibiting MAP kinase phosphatases. *Cell* 2005;120:649–61.

- [55] Kim JH, Rhee JS, Lee JS, Dahms HU, Lee J, Han KN, et al. Effect of cadmium exposure on expression of antioxidant gene transcripts in the river pufferfish, *Takifugu obscurus* (Tetraodontiformes). *Comp Biochem Physiol C Toxicol Pharmacol* 2010;152:473–9.
- [56] Tiron A, Vasilescu C. Role of the spleen in immunity. Immunologic consequences of splenectomy. *Chirurgia* 2008;103:255–63.
- [57] Agnew W, Barnes AC. *Streptococcus iniae*: an aquatic pathogen of global veterinary significance and a challenging candidate for reliable vaccination. *Vet Microbiol* 2007;122:1–15.
- [58] Mitchell P, Tollervey D. mRNA turnover. *Curr Opin Cell Biol* 2001;13:320–5.
- [59] Jang HH, Lee KO, Chi YH, Jung BG, Park SK, Park JH, et al. Two enzymes in one; two yeast peroxiredoxins display oxidative stress-dependent switching from a peroxidase to a molecular chaperone function. *Cell* 2004;117:625–35.
- [60] Kang SW, Rhee SG, Chang TS, Jeong W, Choi MH. 2-Cys peroxiredoxin function in intracellular signal transduction: therapeutic implications. *Trends Mol Med* 2005;11:571–8.
- [61] Ryter SW, Kim HP, Hoetzel A, Park JW, Nakahira K, Wang X, et al. Mechanisms of cell death in oxidative stress. *Antioxid Redox Signal* 2007;9:49–89.